Gas sensing using non-linearly driven polymer-coated quartz crystals.

Mars Geuze *

April 2, 2015

TITLEPAGE

Abstract

abstract

*Advisor: Warner Venstra

Contents

1 Introduction

In our pocket we carry a device which copies almost all human senses. A camera gives your phone sight, a microphone gives your phone ability to hear, and the touch screen is like our skin, allowing your phone to feel touch. The vestibular system is mimicked by a gyroscope and accelerometer combination, and thermoreceptors by thermometers. Using GPS, your phone has a sense of direction, which arguably about half of the human population doesn't even have.

Of course our phone doesn't need the ability to discern flavors, since it is a very picky eater anyway. It only takes electrons at a small range of potentials to get its energy from. But the underlying principle of the senses of taste and smell, namely the ability to detect molecules, can have many more uses than to decide which dish is delicious or foul-tasting. Examples of uses for a nose in your phone would be to test whether you are too intoxicated to drive, or to warn whenever a dangerous amount of carbon-monoxide is in the air. Outside of mobile applications there are even more uses, such as monitoring air quality, indoors or in the city, or more specific in manufacturing plants, stables or greenhouses.

Many devices already exist which can mimic the function of the nose. Notable technologies are gas chromatography and spectroscopy, however these devices are often the size of meters and expensive[XXX]. New methods are needed to decrease the size and cost of an electronic sense of smell. A cheap electric nose which is currently popular is MQ series[XXX]. However, it is weak at discerning molecules and requires six connections per sensor, which makes it cumbersome to use.

XXX something about how usually we try to be linear but we increase sensitivity and resolution with non-linearity.

XXX In this paper the possibility of making a cheap, small nose with a high onderscheidend vermogen XXX is researched. Something about what experiments are described in the paper

2 Theory

2.1 Piezoelectricity

- Cyrstal couples electric field to strain
- Can be modeled by an RLC with CP
- Resonance modes + example

2.2 Crystal oscillator

2.3 Resonance

2.3.1 Q-factor

The Q-factor characterizes a resonators' bandwidth relative to its center resonant frequency. [1]

2.4 Non-linear mechanics

XXX When an electrical potential is applied over a piezoelectric material, the material will deform from its equilibrium position when there is no electrical potential. This results in a restoring force inside the material which opposes the deforming piezoelectric force. The restoring force F can be modeled as a polynomial of the form:

$$F = \sum_{i=1}^{n} -k_i x^i = -k_1 x - k_2 x^2 - \cdots - k_n x^n, \tag{1}$$

where k_n are constants which are to be determined, and x is the displacement due to the deformation. For a symmetric material XXX, the restoring force should have the same magnitude when the deformation is in the positive or in the negative direction. Therefore, the restoring force must be an uneven function, so $k_i = 0$ for even i.

For small displacements, the first term of the restoring force is dominant, and the restoring force can be approximated by Hooke's law choosing $k_i = 0$ for $i \neq 1$:

$$F = k_1 x \tag{2}$$

As displacements become larger, the first term that becomes significant after k_1 is k_3. In this experiment the quartz crystals will be modeled by a system with a restoring force of the form of Equation 1 with only k_1 and k_3 non-zero:

$$F = k_1 x + k_3 x^3. \tag{3}$$

The differential equation for a system with Equation 3 as the restoring force is called the Duffing equation:

$$\ddot{x} + \delta \dot{x} + k_1 x + k_3 x^3 = g(\omega t), \tag{4}$$

where δ determines the amount of damping, k_1 is the linear stiffness, k_3 is the amount of non-linearity in the restoring force and $g(\omega t)$ is a driving function with frequency ω.

2.5 Solving the Duffing equation

XXX some derivation of the frequency curve.

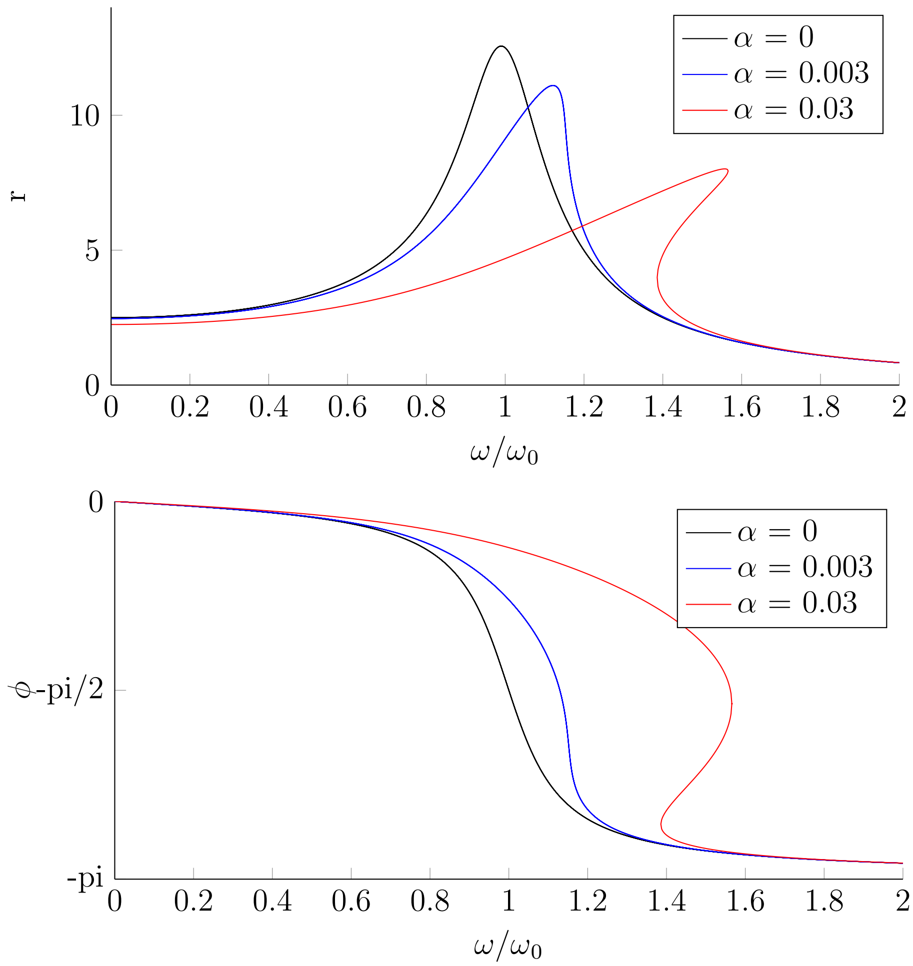

Figure 1: Frequency response of the Duffing equation with $\epsilon = 1$, $\delta = 0.2$, $\gamma = 2.5$ for different values of non-linearity α. With higher non-linearity, the curve becomes less symmetric and at high enough values for α, multiple solutions are possible for a given frequency.

3 Method & Materials

We start a basic description and simulation of the measurement setup. Subsequently, the basic characterization of a quartz crystal is researched and we proceed to experiment with its amplitude-frequency dependence. Afterwards, the crystal is coated, and the behavior of the system with the introduction of different chemical compounds is investigated.

3.1 Experimental set-up

The set-up consists of the electrical system to drive the crystals and measure its response, and of the system to bring the coated crystals in contact with gasses. The two systems will be described consecutively in the following sections.

3.1.1 Electrical system

A basic overview of the electrical system is shown in Figure 2. The signal of a lock-in amplifier is amplified and buffered before exciting the crystal. The current is probed and this signal is fed back into the lock-in amplifier to measure the response of the crystal. The current flowing through the crystal is indicative of the impedance of the crystal, and thus whether the crystal is in resonance. For a detailed schematic and an overview of all used components, see **??**

3.2 Crystal analysis

The goals of the first phase are to choose a resonator and find benchmark impedance-frequency data of the chosen resonator.

Since a mechanical resonator is needed to react to the change of mass, but it is desirable to drive and analyze the system electronically, a piezoelectric resonator is used as a transformer between the electronic and mechanical signal. Piezoelectric devices exist with a Q-factor of up to XXX, but they are very expensive. Ceramic resonators are cheap, but they lack stability and have low Q-factors XXX. A good middle ground is a quartz crystal oscillator, since they have Q-factors up to 10^6, and are readily available because of their use in almost any electronic device on the market.

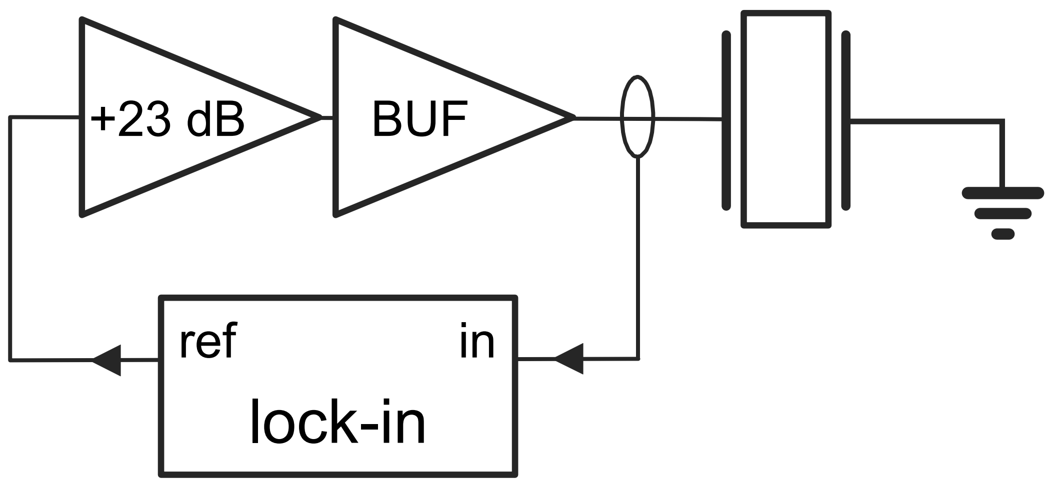

Figure 2: Schematic overview of the electrical system of the experimental set-up.

Quartz crystals come in a variety of fundamental frequencies, shapes and sizes. For this experiment a large crystal is preferred over a small crystal, since it eases polymer coating. The fundamental frequency is preferably small, since it loosens bandwidth requirements of all components in the circuit and reduces crosstalk and phase lag XXX. The most common crystal shapes are a planar shear resonator and a tuning fork. Since the tuning fork has an irregular shape, it is hard to get an even coating. The first tests resulted in a coating which filled up the gap XXX.

The circuit used in the first test is

3.2.1 Measurement

Since the crystal is driven by a voltage

3.3 Gas mixture set-up

To measure the response of the coated quartz crystals to gasses, a setup is needed to put the quartz crystal inside a gas mixture. The most important parameters of the gas mixture are the homogeneity, the accuracy of the mixing ratio and the pressure. It is possible to make a gas mixing set-up, but gas mixtures specifically for gas sensor calibration are available on the market as well. The calibration mixtures would have a higher concentration accuracy, whereas the gas mixture setup would have a higher flexibility. When using off-the-shelve gas mixtures, a new pre-made gas mixture would have to be bought. Therefore a gas mixing set-up will be made.

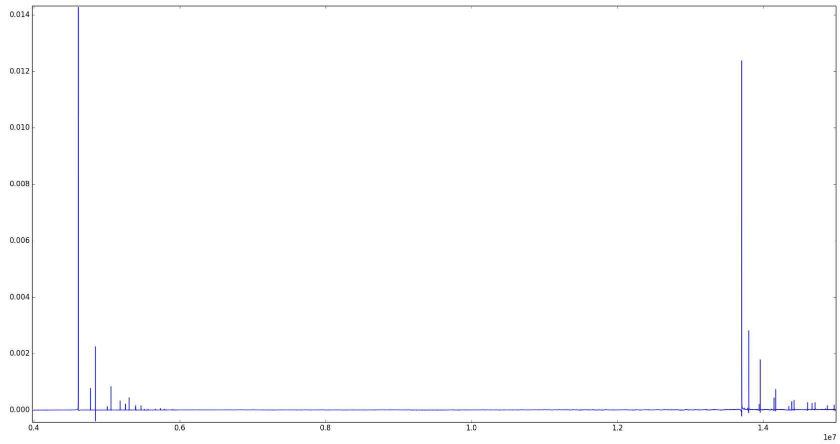

Figure 3: Frequency scan of the crystal.

4 Results & Discussion

4.1 Orientation

The frequency scan in Figure 3 shows that apart from the large resonance peak at the crystal manufacturer's stated resonance frequency of $f_0 = 4.606\,\text{MHz}$, there are many smaller peaks corresponding to different resonance modes. The largest response is not necessarily the most useful response for this experiment.

First of all, a large response means a high current. Apart from the difficulty of making a high frequency source with high current, this leads to several undesirable effects, such as heating up of the crystal [XXX] and high voltage drops in parasitic inductances. When several crystals are paralleled, their currents are summed, which further increases the effect of the parasitic inductance.

Secondly, the level of amplitude-frequency dependence seems to be independent of the size of the response. A high level of amplitude-frequency dependence is desirable, since lower amplitudes are needed to reach bistability, which eases the requirements of the driving system. It is also expected that a high level of amplitude-frequency dependence leads to a higher sensitivity to mass XXX.

Finally, not only do the characteristics of the resonance peak itself (i.e. its size and its amplitude-frequency dependence) matter, but also how far it is from its other resonance peaks. Since the crystals will be paralleled, a large area without resonance peaks around the peak that is used for measurement is needed to limit the amount of crosstalk.

The resonance peak at $f = 4.8\,\mathrm{MHz}$ [XXX] was selected to use for the rest of this experiment. The peak has a significant amplitude-frequency dependence, while having an amplitude of about 6 times lower than the large main resonance peak at $f_0 = 4.606\,\mathrm{MHz}$.

4.2 Amplitude-frequency dependent behavior experiment

A few frequency responses of an uncoated crystal at different driving powers can be found in Figure 4. The crystal shows linear behavior at low driving amplitudes, but it becomes bistable as the driving amplitude rises. The bistable area in Figure 5 is obtained by subtracting the response of the backward sweep from the response of the forward sweep.

In Figure 6 some frequency sweeps at different driving powers of four identical crystals with different coatings (PDMS, PEG, PEE and PAA) are displayed alongside their responses before coating. The coating has decreased the resonance frequency of the crystal, as was expected due to mass loading. The Q-factor has also decreased, which can be attributed to losses in the coating. A third observation is that the amplitude-frequency dependence has decreased. This can be explained by the lower Q-factor. The amplitude of mechanical movement, and therefore the significance of non-linear effects, is smaller due to the higher damping. The new bistable areas can be found in Figure 7, alongside their old bistable areas in dashes.

Figure 8 shows the frequency response at a constant driving amplitude of four crystals with closely spaced resonance frequencies placed in parallel, alongside the four individual responses of the crystals. The jump points of the parallel response are to the jump points of the individual crystals, but not quite identical. There are two factors which give rise to this behaviour. Firstly there will always be some crosstalk between the crystals, since the driving circuit is not a perfect voltage source. Secondly, since this experiment is conducted in open air, fluctuations in temperature and humidity are responsible for a different outcome of each measurement.

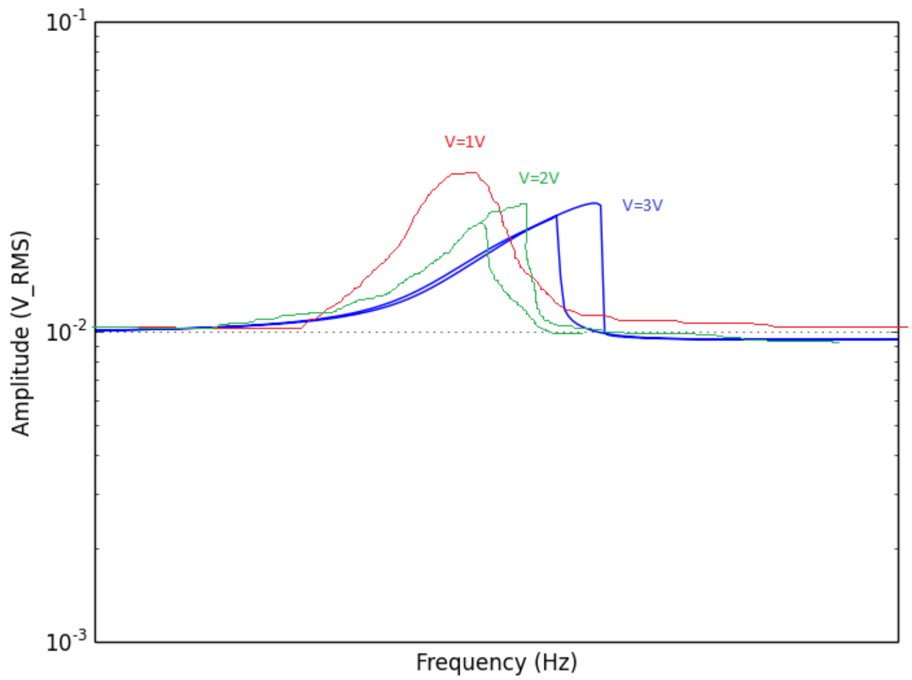

Figure 4: Some sweeps at different power XXX

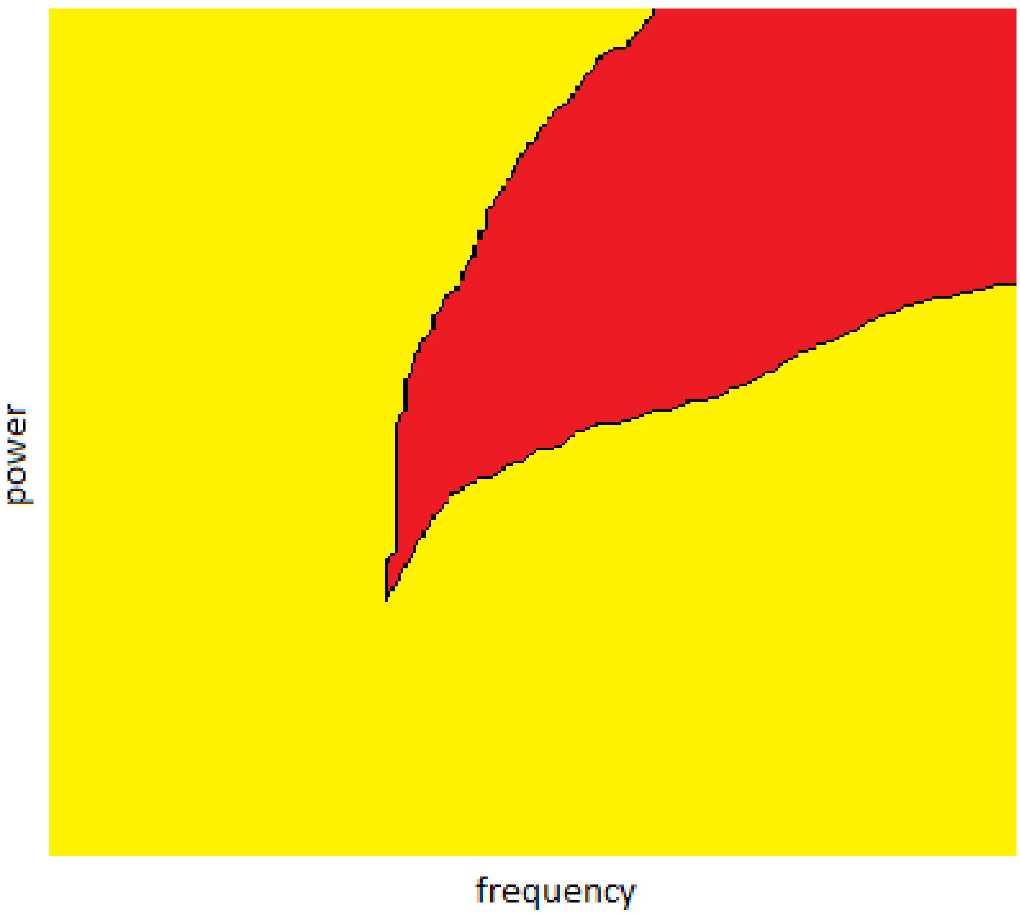

Figure 5: Hysteresis plot of XXX

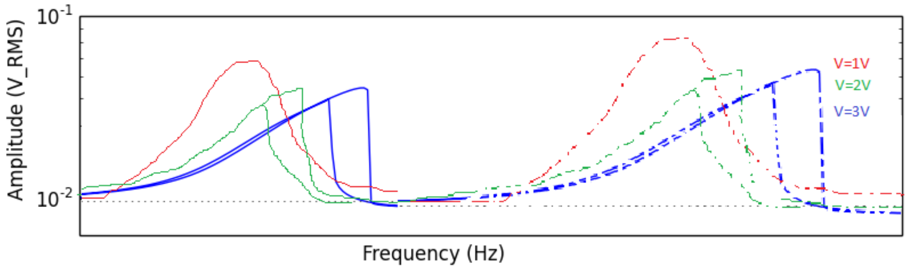

(a) PDMA

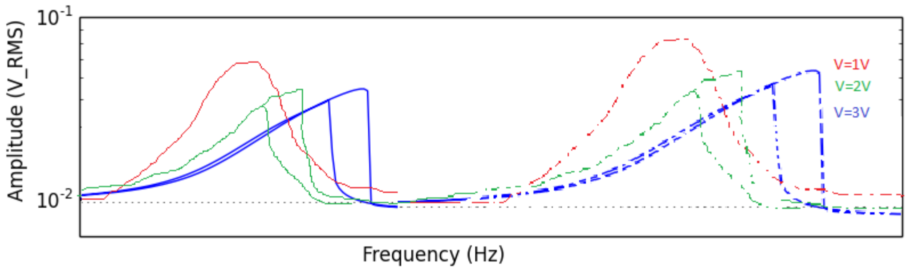

(b) PEG

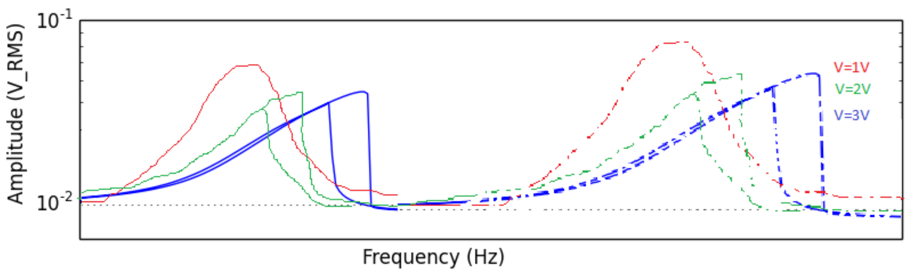

(c) PEE

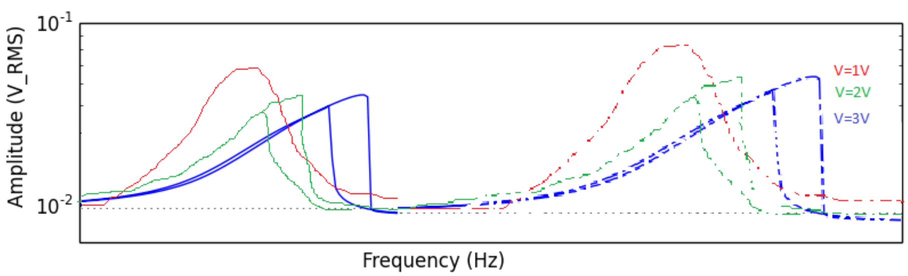

(d) PAA

Figure 6: A few frequency responses of four identical crystals with different coatings alongside their original responses before coating (dashed).

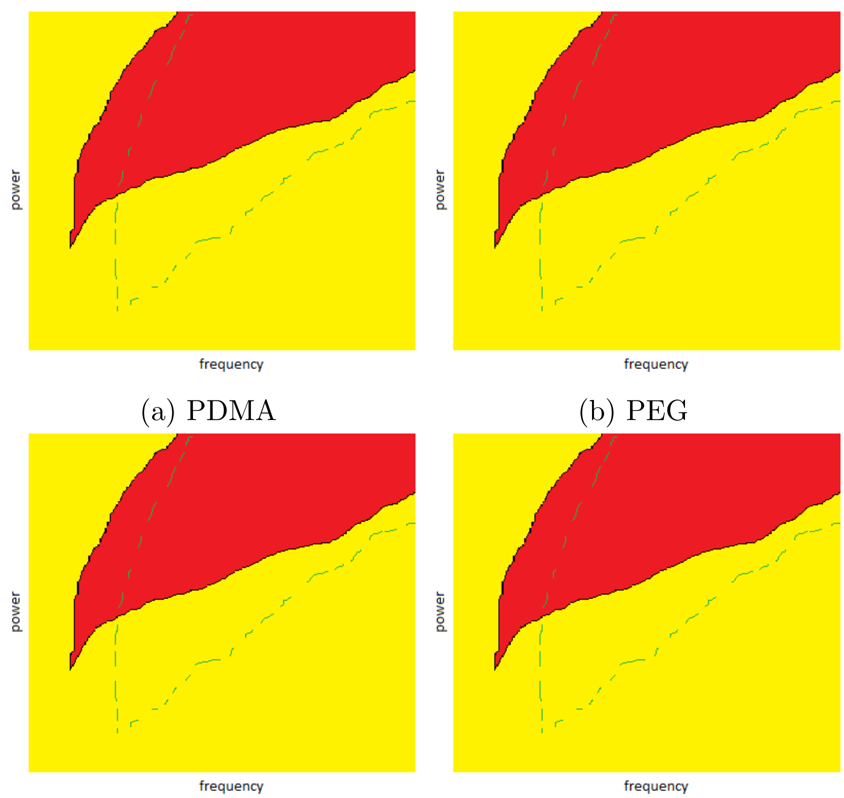

(a) PDMA (b) PEG

(c) PEE (d) PAA

Figure 7: Bistable regime before (dashed) and after coating for four identical crystals with different coatings.

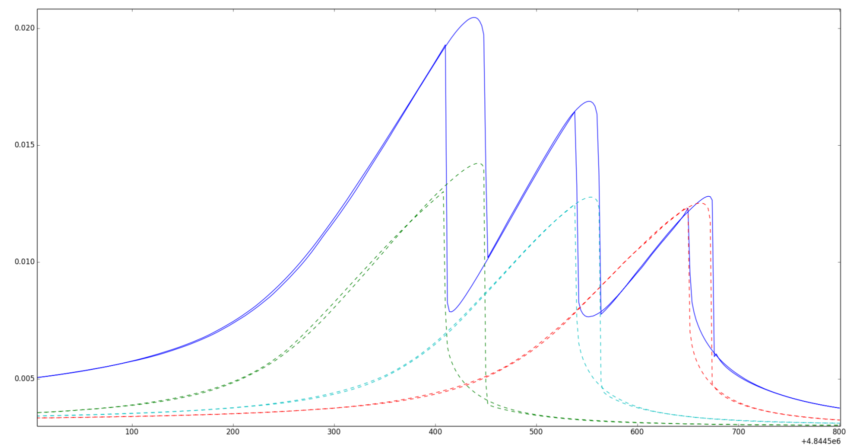

Figure 8: The frequency response of three parallel uncoated crystals with closely spaced resonance frequencies. The driving amplitude is $V_p = 3.25\,\mathrm{V}$. The frequency responses of the individual crystals are dashed.

As the jump points of the frequency response will shift when a gas is sensed, the crosstalk will manifest itself differently for different mixtures of gasses, so it will always degrade the measurement in an unpredictable way. The error due to fluctuations in temperature and humidity can be minimized by repeating the measurement and averaging the results.

4.3 Gas sensing

5 Conclusion

Biochemical Sensors: Mimicking Gustatory and Olfactory Senses

References

[1] Michael H. Tooley. *Electronic circuits: fundamentals and applications.* Elsevier, 2006.

A Detailed electrical system

The voltage drop over a series shunt resistor is measured using a differential amplifier. This voltage drop, which is linearly proportional to to the current that flows through the quartz crystal as described by Ohm's law, is indicative of the changing impedance of the crystal as a function of frequency. Therefore, this signal can be used to show when the crystal is on resonance.

A more detailed schematic can be found in Figure 9. Preliminary tests showed that the peak voltage of about $V_p = 10$ V is needed to see a significant amplitude-frequency dependence. The maximum current at this voltage is about $I_p = 200$ mA. A high speed operational amplifier was used in combination with a buffer amplifier in the feedback path to decrease the output impedance and increase the output current capability of the amplifier. The slew rate of the amplifier is also an important parameter, since the signal has both high frequency and high amplitude. The needed slew rate corresponds to the maximum slope of the output signal, which for a sinusoidal signal of the following form:

$$v(t) = V_P \sin 2\pi f t, \tag{5}$$

is given by:

$$\max\left(\left|\frac{dv(t)}{dt}\right|\right) = \frac{\pi f V_P}{2}. \tag{6}$$

Using crystal frequency of $f = 4.606\,\mathrm{MHz}$ and a peak voltage of $V_p = 10$ V, the minimum slew rate of the amplifier should therefore be $425\,\mathrm{V/\mu s}$.

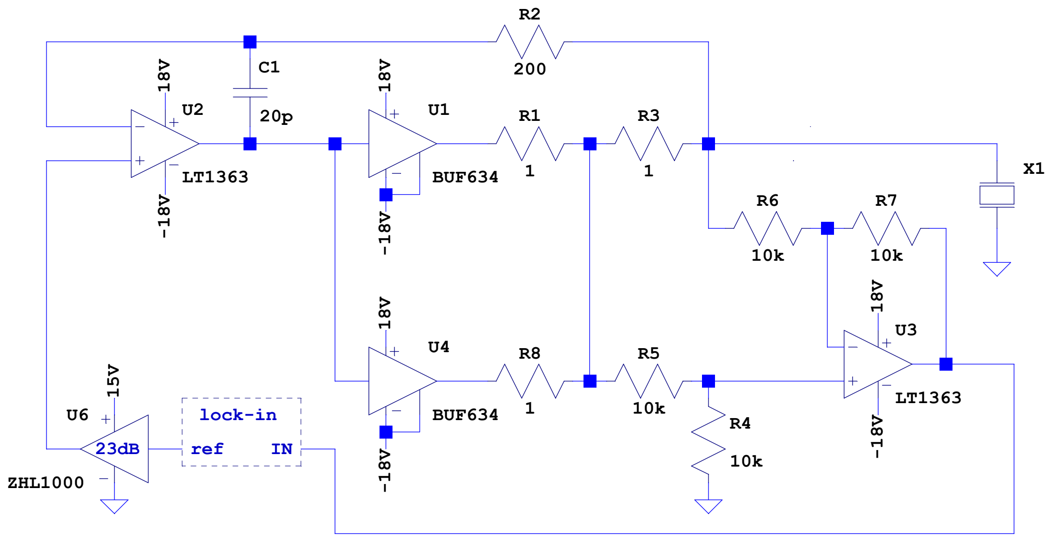

Figure 9: Detailed schematic of the electrical system of the experimental set-up.

B Temperature-based quartz crystal relaxation oscillator